PNAS RESEARCH ARTICLE | APPLIED BIOLOGICAL SCIENCES OPEN ACCESS

Enhanced production of acetyl-CoA-based products via peroxisomal surface display in *Saccharomyces cerevisiae*

Hannah C. Yocum[a,1], Shane Bassett[a,1], and Nancy A. Da Silva[a,2]

Edited by Sang Yup Lee, Korea Advanced Institute of Science and Technology, Daejeon, Korea (South); received August 31, 2022; accepted October 28, 2022

Colocalization of enzymes is a proven approach to increase pathway flux and the synthesis of nonnative products. Here, we develop a method for enzyme colocalization using the yeast peroxisomal membrane as an anchor point. Pathway enzymes were fused to the native Pex15 anchoring motif to enable display on the surface of the peroxisome facing the cytosol. The peroxisome is the sole location of β-oxidation in *Saccharomyces cerevisiae,* and acetyl-CoA is a by-product that is exported in the form of acetyl-carnitine. To access this untapped acetyl-CoA pool, we surface-anchored the native peroxisomal/mitochondrial enzyme Cat2 to convert acetyl-carnitine to acetyl-CoA directly upon export across the peroxisomal membrane; this increased acetyl-CoA levels 3.7-fold. Subsequent surface attachment of three pathway enzymes – Cat2, a high stability Acc1 (for conversion of acetyl-CoA to malonyl-CoA), and the type III PKS 2-pyrone synthase – demonstrated the success of peroxisomal surface display for both enzyme colocalization and access to acetyl-CoA from exported acetyl-carnitine. Synthesis of the polyketide triacetic acid lactone increased by 21% over cytosolic expression at low gene copy number, and an additional 11-fold (to 766 mg/L) after further optimization. Finally, we explored increasing peroxisomal membrane area through overexpression of the peroxisomal biogenesis protein Pex11. Our findings establish peroxisomal surface display as an efficient strategy for enzyme colocalization and for accessing the peroxisomal acetyl-CoA pool to increase synthesis of acetyl-CoA-based products.

peroxisomal surface display | PEX15 | acetyl-CoA | polyketides

Significance

Colocalization of pathway enzymes is a proven method to increase pathway flux and the synthesis of nonnative products. Here we detail a method of colocalization that both uses the peroxisomal membrane surface as an anchoring site and enables capture of peroxisomal acetyl-CoA. Display of the native peroxisomal/mitochondrial enzyme Cat2, to intercept exported acetyl-carnitine for conversion back to acetyl-CoA at the membrane surface, significantly increased acetyl-CoA levels. The production of a polyketide (using three peroxisome-bound pathway enzymes) also increased, demonstrating the effectiveness of this display strategy for both colocalization and accessing peroxisomal acetyl-CoA. This method can be used to colocalize any small pathway, and with the anchoring of Cat2, can be applied to increase the synthesis of other acetyl-CoA-based products.

Biosynthesis, which harnesses microbial metabolism to produce desired compounds, has many advantages over traditional chemical synthesis, including greater economic viability and a much lower carbon footprint (1–3). This has led to the use of microorganisms in industrial biomanufacturing for production of a wide range of natural products, including those related to the pharmaceutical, food, agriculture, and petrochemical industries. Polyketides are one such class of natural products that span all of these industries, with their main appeal as pharmaceuticals due to their antimicrobial, anticancer, and immunosuppressive properties (4). Polyketides have been reported to comprise over 20 billion USD in the annual pharmaceuticals market and account for over a third of all natural product-derived drugs approved by the United States Food and Drug Administration (5–7). Biosynthesis of these molecules is via polyketide synthases (PKS) that use the central metabolite Coenzyme A (CoA) species (e.g., acetyl-CoA, propionyl-CoA, and malonyl-CoA) as building blocks. Triacetic acid lactone (TAL) is a simple polyketide that can be synthesized in yeast from acetyl-CoA and malonyl-CoA via the *Gerbera hybrida* type III 2-pyrone synthase (2-PS) (8, 9) and is considered a platform chemical that can be converted to a wide range of high-value and commodity products (10, 11). TAL is also easily assayed, making it effective for identifying microbial strains with the optimized acetyl- and malonyl-CoA pools needed for production of higher order polyketides and other acetyl-CoA-based products.

Acetyl-CoA is readily formed in yeast in four intracellular locations: the nucleus, the cytosol, the mitochondria, and the peroxisome (12), with acetyl-CoA diffusing freely between the cytosol and the nucleus (13). For polyketide production in the cytosol of the yeast *Saccharomyces cerevisiae*, strategies to increase acetyl-CoA (e.g., pathway engineering, reducing the transport of pyruvate and acetyl-CoA into the mitochondria) have successfully increased TAL levels (8, 14, 15). The peroxisome is the sole location of β-oxidation in *S. cerevisiae*, breaking down fatty acids and converting them into acetyl-CoA (16). Localizing pathways within the peroxisome has been used to improve the synthesis of fatty acids and fatty alcohols (17, 18), alkanes (18), and isoprenoids (19, 20), products made from acetyl-CoA. However, utilizing the peroxisomal acetyl-CoA in the cytosol poses a challenge, as acetyl-CoA cannot pass through the peroxisomal membrane. The acetyl-CoA produced by β-oxidation is instead exported from the organelle in the form of

Author contributions: H.C.Y., S.B., and N.A.D.S. designed research; H.C.Y. and S.B. performed research; H.C.Y., S.B., and N.A.D.S. analyzed data; and H.C.Y., S.B., and N.A.D.S. wrote the paper.

The authors declare no competing interest.

This article is a PNAS Direct Submission.

[1]H.C.Y. and S.B. contributed equally to this work.

[2]To whom correspondence may be addressed. Email: ndasilva@uci.edu.

This article contains supporting information online at https://www.pnas.org/lookup/suppl/doi:10.1073/pnas.2214941119/-/DCSupplemental.

Published November 21, 2022.

acetyl-carnitine, a conversion catalyzed by the *S. cerevisiae* mitochondrial/peroxisomal carnitine acetyl-CoA transferase (Cat2), for transport and subsequent use in the mitochondria (21). To capture acetyl-CoA produced in the peroxisome for cytosolic polyketide synthesis, the acetyl-carnitine should be rapidly converted back to acetyl-CoA following the exit from the peroxisome. A simple strategy would be to express the mitochondrial/peroxisomal Cat2 in the cytosol. Given the bidirectionality of Cat2 catalysis, cytosolic expression could result in acetyl-carnitine interception enroute to the mitochondria and therefore increased acetyl-CoA levels.

Peroxisomal biogenesis, general peroxisomal maintenance, and the import and export of proteins and metabolites are mediated by a handful of membrane proteins called peroxins (22). The Pex15 peroxin is a tail-anchored protein, comprised of a single transmembrane domain and a C-terminal anchoring motif used for docking and membrane translocation with Pex19 (23–25). Previous work isolated the C-terminal 68 amino acid (aa) chain of Pex15 used for membrane docking to the peroxisome surface, and demonstrated that fusion of this C-terminal peptide to GFP or the mitochondrial Fis1 resulted in localization of these proteins on the cytosolic side of the peroxisomal membrane (24). Fusion of this sequence with the native Cat2 could thus be used for interception of the exported acetyl-carnitine at the peroxisomal surface for immediate conversion back to acetyl-CoA, increasing acetyl-CoA levels in the cytosol. Furthermore, the fusion of the Pex15 peptide to multiple pathway enzymes could create a unique method for enzyme colocalization; the close anchoring of enzymes allows for increased flux to the desired product (26).

In this study, the 68 aa Pex15 C-terminal anchoring motif (PEX15) was used to colocalize enzymes on the surface of the peroxisomes to both improve metabolic pathway flux and to enable the use of the peroxisomal acetyl-CoA pool in *S. cerevisiae*. We first anchored the *S. cerevisiae* Cat2 enzyme and demonstrated significantly higher cytosolic acetyl-CoA levels. We then anchored three enzymes as a metabolon for the synthesis of the polyketide TAL: the Cat2 enzyme to produce the starter unit acetyl-CoA, a stable *S. cerevisiae* acetyl-CoA carboxylase ($Acc1^{S1157A}$) for conversion of acetyl-CoA to the extender unit malonyl-CoA (27), and the *G. hybrida* 2-PS for TAL synthesis. Increases in TAL demonstrated the success of our strategy. Finally, we explored varying the peroxisomal membrane surface area through the overexpression of the peroxisomal biogenesis protein Pex11, which results in an increased number of smaller peroxisomes, greater membrane area, and the stimulation of β-oxidation (28–30). The research establishes a new approach to enzyme colocalization within the cytoplasm of yeast and a means to access the untapped peroxisomal acetyl-CoA pool for improved production of polyketides and other acetyl-CoA-based products.

Results

Accessing Acetyl-CoA from the Yeast Peroxisome. Advantages of peroxisomal surface localization include both increasing pathway flux via enzyme proximity and the ability to exploit the peroxisomal acetyl-CoA exported from the peroxisome in the form of acetyl-carnitine. We first overexpressed free or anchored Cat2 to capture and convert this acetyl-carnitine to acetyl-CoA, and evaluated the impact on acetyl-CoA levels in the cell. Cat2 or Cat2 directly fused to the PEX15 anchoring motif (Cat2PEX15) was expressed using the strong *S. cerevisiae TEF1* promoter on CEN/ARS plasmids. These plasmids, along with an empty plasmid (no Cat2), were independently transformed into base strain BY4741, and cultures were grown for 48 h before acetyl-CoA extraction and analysis (14).

A significant increase in specific acetyl-CoA titer was observed as we moved from no additional Cat2 expression to unanchored Cat2 expression to anchored Cat2 expression (Fig. 1*A*). Direct fusion of Cat2 to PEX15 was chosen as incorporating a linker reduced performance (*SI Appendix*, Fig. S1). Expression of Cat2 alone improved specific acetyl-CoA levels 2.2-fold over basal levels, with an additional 1.7-fold improvement when the Cat2 was anchored to the peroxisome surface (Fig. 1*A*). This is consistent with what was expected. Expression of Cat2 should increase acetyl-CoA levels as the enzyme can intercept acetyl-carnitine enroute to the mitochondria. Peroxisomal surface display of Cat2 should result in a further increase in acetyl-CoA as Cat2 can intercept acetyl-carnitine immediately upon export from the peroxisome (Fig. 1*B*). No significant changes in cell densities were observed between any two groups (*SI Appendix*, Fig. S1*A*); thus, the overall

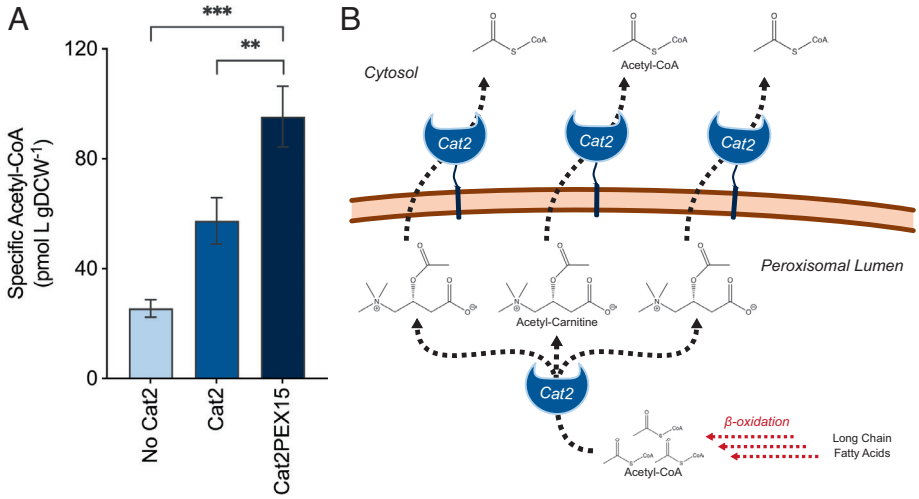

Fig. 1. Access to peroxisomal acetyl-CoA pools through interception by Cat2. (*A*) Specific acetyl-CoA levels were measured using a fluorescence-based assay and normalized to final cell densities; higher acetyl-CoA levels were observed for the strains expressing the Cat2-encoded carnitine acetyl-CoA transferase, particularly for Cat2 anchored to the peroxisome surface. (*B*) Schematic illustrating how acetyl-CoA is converted into acetyl-carnitine for transport to the mitochondria, and then subsequently converted back to acetyl-CoA by Cat2 proteins displayed on the surface of the yeast peroxisome. Bars represent mean ± 1-SD, $n = 3$ biological replicates, $^{**}P < 0.01$, $^{***}P < 0.001$.

3.7-fold increase for Cat2PEX15 relative to the control demonstrates the ability of peroxisomal display of Cat2 to access the untapped peroxisomal acetyl-CoA pool and should prove beneficial for the synthesis of polyketides and other acetyl-CoA-based products.

Peroxisomal Display of Three Enzymes for Synthesis of Acetyl-CoA-Based Product TAL. We next evaluated peroxisomal display using a 3-enzyme metabolon for TAL synthesis: *S. cerevisiae* Cat2, *S. cerevisiae* Acc1^{S1157A} (Acc1m), and the *G. hybrida* 2-PS. In this configuration, the Cat2 on the peroxisome surface will intercept the acetyl-carnitine exported from the peroxisome and convert it to acetyl-CoA for immediate use by the coanchored Acc1m and 2-PS. Acc1m was chosen as the S1157A mutation prevents enzyme deactivation after glucose depletion (27), enabling higher polyketide synthesis. Anchoring all three enzymes on the surface of the peroxisome should create an enzyme cascade that increases the synthesis of TAL. We evaluated how anchoring the Cat2, Acc1m, and 2-PS enzymes alone and in combination affects TAL production and compared this with free enzymes in the cytosol (Fig. 2 *A* and *B*).

We first checked TAL production with Acc1m fused directly to PEX15 or via a short flexible linker; as with Cat2, no improvement was observed with the linker (*SI Appendix*, Fig. S2). Direct fusion of PEX15 to 2-PS also did not reduce TAL levels (*SI Appendix*, Fig. S3). We thus proceeded with all three enzymes directly fused to PEX15. An increase in cell density and TAL titer was also observed between 48 and 96 h (*SI Appendix*, Fig. S2), so we chose the longer cultivation time. This should also benefit expression of the full pathway; additional culture time should allow the cells to consume larger amounts of fatty acids, leading to an increase in acetyl-CoA available for TAL synthesis from β-oxidation in the peroxisome.

To avoid the instability and metabolic burden imposed by multiple plasmids, the genes for 2-PS or the 2-PSPEX15 fusion were integrated into chromosomal site XI-3 (31) of strain BY4741 resulting in strains BY2PS and BY2PSP, respectively. The genes for Cat2, Acc1m, or their PEX15 fusions were inserted alone or in combination on a single low-copy bicistronic CEN/ARS plasmid, with all genes expressed under the control of *TEF1* promoters. This should result in similar expression levels of the three pathway enzymes (with gene copy numbers of approximately 1:1.5:1.5). Strains BY2PS and BY2PSP were transformed with an empty plasmid or the plasmid carrying Cat2, Cat2PEX15, Acc1m, Acc1mPEX15, Cat2 and Acc1m, or Cat2PEX15 and Acc1mPEX15. The addition of Cat2 or Cat2PEX15 to strain BY2PSP did not increase specific TAL titers (Fig. 2*C*). This was not surprising; while acetyl-CoA levels increase (Fig. 1*A*), both acetyl-CoA and malonyl-CoA are required for TAL synthesis, and Acc1 is often limiting (27, 32). Accordingly, the addition of free or anchored Acc1m alone resulted in significantly higher specific titers. The anchoring of both Cat2 and Acc1m in strain BY2PSP resulted in a further increase in TAL; with all three enzymes anchored, there was a 2.3- to 2.8-fold increase relative to targeted 2-PSPEX15 or cytosolic 2-PS alone, and a 21% increase relative to all three enzymes cytosolically expressed. Cell densities remained

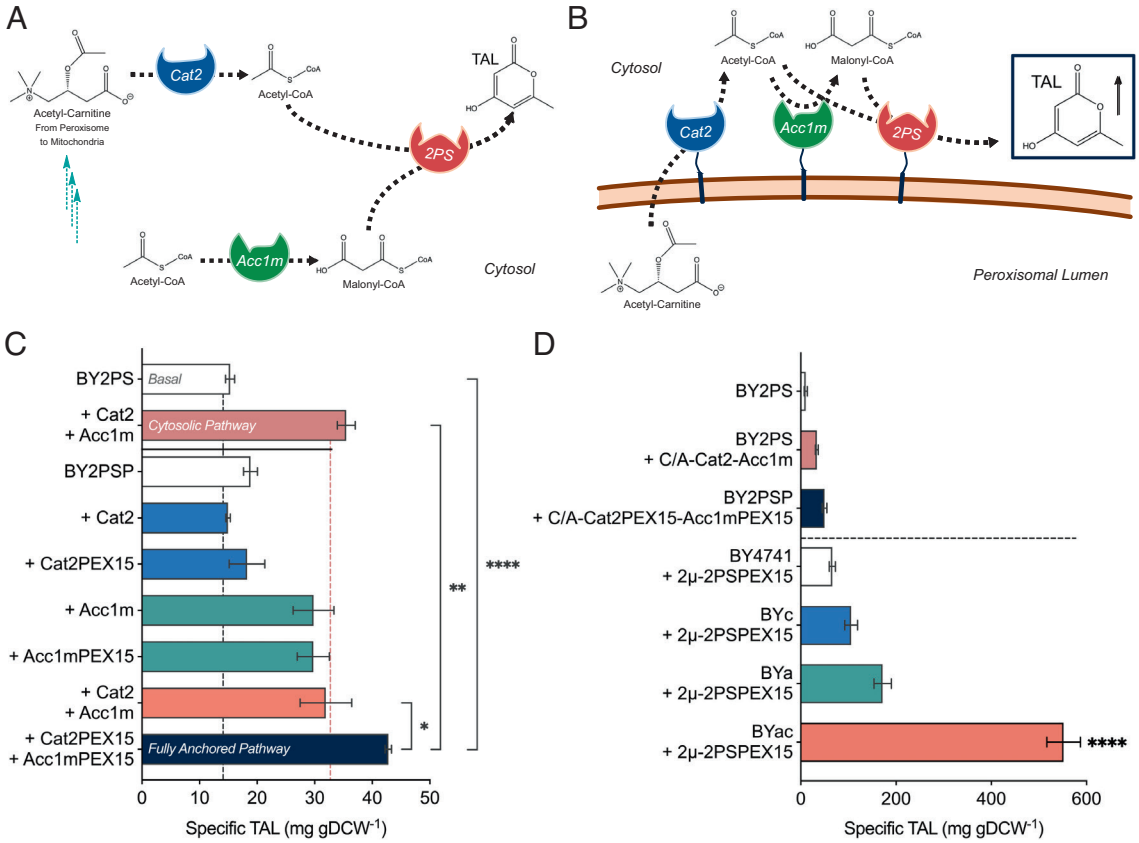

Fig. 2. Improving polyketide biosynthesis through peroxisomal surface display and increased 2-PS expression. Schematics for (*A*) a cytosolic pathway and (*B*) a peroxisomal bound pathway. (*C*) TAL titers normalized to final cell densities for free and anchored Cat2, Acc1m, and/or 2-PS enzymes. Each enzyme is introduced at 1–2 copies (2-PS or 2-PSPEX15 was integrated at one copy; Cat2, Acc1m, their PEX15-bound fusions, and enzyme combinations were carried on low-copy CEN/ARS bicistronic plasmids). (*D*) Pathway optimization with Cat2PEX15 and Acc1mPEX15 integrated at one copy and 2-PSPEX15 on a multicopy 2μ plasmid significantly improved TAL titers. Bars represent mean ± 1-SD, $n = 3$ biological replicates, $^*P < 0.05$, $^{**}P < 0.01$, $^{****}P < 0.0001$.

unchanged across these experimental groups (*SI Appendix*, Fig. S3*A*). The results demonstrate the success of enzyme colocalization on the peroxisome for a pathway designed to utilize the exported acetyl-carnitine from β-oxidation.

An interesting trend is observed in a similar experiment with unanchored 2-PS (*SI Appendix*, Fig. S3). Again, specific TAL titers remain relatively unchanged (and similar for both anchored and unanchored 2-PS) when either Cat2 or Acc1 is individually anchored. However, when Acc1m and Cat2 are both anchored, TAL titer is significantly lower for free 2-PS relative to 2-PSPEX15. Anchoring of Acc1m and Cat2 together may effectively shift the location of available acetyl-CoA and malonyl-CoA needed for TAL synthesis away from the 2-PS in the bulk cytosol. Thus 2-PS must also be anchored to see the >2-fold improvement over basal levels.

Optimizing Pathway Configuration for Improved Polyketide Synthesis via Peroxisomal Display. Our initial system had only one integrated copy of 2-PSPEX15 and a 15-kb CEN/ARS vector (1–2 copies) carrying Acc1mPEX15 and Cat2PEX15. To ensure stable expression, we integrated the genes for Cat2PEX15 and Acc1mPEX15 into the BY4741 genome at sites XI-3 and XI-5, respectively, resulting in strain BYac. Control strains had either no integrations (base strain BY4741) or only one of the two genes (strains BYa and BYc). Based on our previous work showing higher TAL levels with increased 2-PS gene copy number (8), we chose to express 2-PSPEX15 from a multicopy 2μ plasmid to take full advantage of our anchored system. We then compared specific TAL titer after 96 h of cultivation for each of the four multicopy 2-PSPEX15 strains and also relative to three strains from our initial low-copy system (Fig. 2*D*).

Increasing copy number of 2-PSPEX15 increased specific TAL titer 3.5-fold over low-copy chromosomal expression (BY2PSP). The integration of the genes for Cat2PEX15, Acc1mPEX15, or both proteins resulted in an increase in the specific TAL titer with each intervention. Integrating Cat2PEX15 and Acc1mPEX15 individually resulted in a 1.6- and a 2.6-fold increases, respectively. With both genes integrated (strain BYac + 2μ-2PSPEX15) and thus all three enzymes on the peroxisome surface, the highest TAL titers were observed reaching 766 ± 13 mg/L, a sizeable increase ranging from 1.2- to 4.7-fold compared with all other strains tested (*SI Appendix*, Fig. S4). Normalized to cell densities, this constituted an 8.3-fold increase in TAL production relative to BY4741 + 2μ-2PSPEX15, and an 11-fold increase relative to our low-copy fully anchored pathway (Fig. 2 *C* and *D*).

The overall fitness of the final strains was affected when both Cat2 and Acc1m were localized on the peroxisome. With 2-PS or 2-PSPEX15 expressed from the multicopy plasmid, strains BY4741, BYc, and BYa all reached similar final cell densities, while BYac had a cell density 40% lower (*SI Appendix*, Fig. S4). This is due to the colocalization of Cat2 and Acc1m, as this drop in cell density is observed with both anchored and free 2-PS (*SI Appendix*, Fig. S4). Even so, the highest TAL levels (both specific titer and total titer) were observed when all three enzymes were anchored on the surface and with high-copy expression of 2-PS (Fig. 2 and *SI Appendix*, Fig. S4). Our results thus confirm that pathway display on the surface of the peroxisome is advantageous due to both enzyme colocalization and access to the peroxisomal acetyl-CoA pool (via Cat2) and provides for high-level production of acetyl-CoA-based products like polyketides.

Improving Polyketide Synthesis Through Alterations of Peroxisome Surface Area. Yeast peroxisomes are typically 0.1 and 0.2 μm in diameter, with only about 2–3 peroxisomes per cell in wild-type *S. cerevisiae* (33). Peroxisomal biogenesis is mediated by a handful of membrane proteins called peroxins, facilitating elongation, constriction, and fission of new peroxisomes from mature ones. These peroxins also play a role in regulating the number and size of peroxisomes (22). One of these peroxins, Pex11, is exceptionally important in both peroxisome proliferation and regulation of β-oxidation; previous reports have cited an increased number of small peroxisomes in strains with *PEX11* overexpression (28, 29). Furthermore, overexpression of *PEX11* in *S. cerevisiae* has been shown to accelerate β-oxidation, leading to greater availability of acetyl-CoA in these organelles (30).

To determine how the performance of our anchored system is affected by reduced peroxisome size, greater membrane surface area (30), and increased β-oxidation, we created strains overexpressing *PEX11*. The Pex11 gene was amplified from BY4741 genomic DNA and inserted (under the control of the *TEF1* promoter) along with the 2-PSPEX15 gene on either low-copy CEN/ARS or 2μ bicistronic plasmids. Overexpressing *PEX11* simultaneously with 2-PSPEX15 on the 2μ plasmid did not significantly affect TAL titers relative to the control strain (*SI Appendix*, Fig. S5). This is expected as only 2-PS is anchored; precursor levels or availability have not been changed. For 2-PSPEX15 on the CEN/ARS plasmid, however, a 29% reduction in TAL titer was observed (*SI Appendix*, Fig. S5). Overexpressing *PEX11* increases the number and reduces the size of the peroxisome; with the

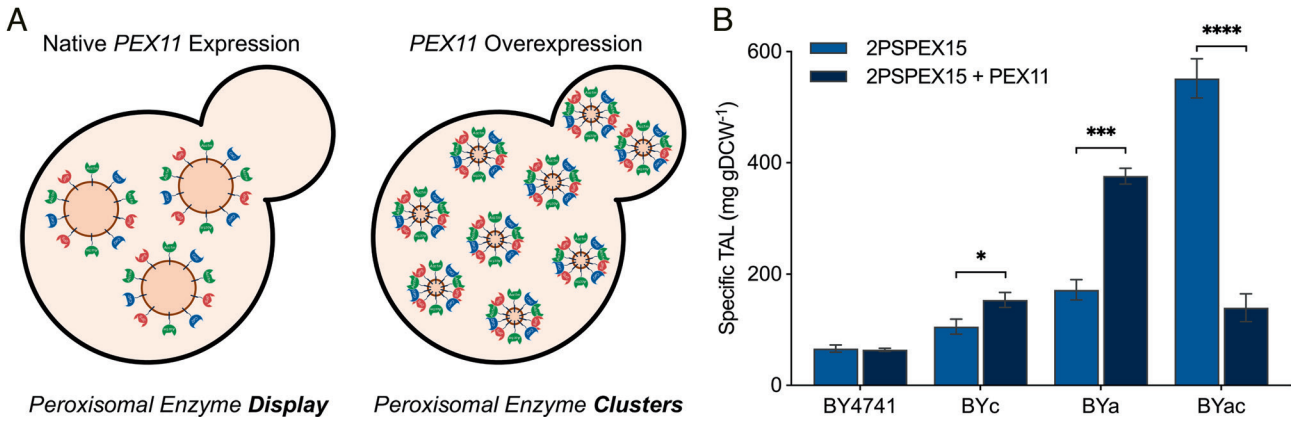

Fig. 3. Effects of Pex11 overexpression on TAL synthesis. (*A*) Schematics for native and for overexpression of the peroxisomal biogenesis *PEX11* gene illustrate the change in size, number, and overall surface area of the yeast peroxisomes. (*B*) TAL titers normalized to cell densities for strains BY4741, BYc, BYa, and BYac expressing 2-PSPEX15 or both 2-PSPEX15 and Pex11 from a multicopy 2μ plasmid. Bars represent mean ± 1 SD, $n = 3$ biological replicates, *$P < 0.05$, ***$P < 0.001$, ****$P < 0.0001$.

increased membrane area (30) and low 2-PSPEX15 expression, 2-PS dimerization (required to form a fully functional active site for biocatalysis (34)) may be inhibited.

We then evaluated the effect of *PEX11* overexpression on the TAL titer for our fully anchored system (Fig. 3*A*). The multicopy 2μ plasmids carrying 2-PSPEX15 alone or 2-PSPEX15 and *PEX11* were each transformed into strains BY4741, BYc, BYa, and BYac. The strains were cultivated for 96 h before TAL analysis. For BYc (Cat2 anchored) expressing 2-PSPEX15, the addition of Pex11 overexpression increased the specific TAL titer (Fig. 3*B*) with no effect on the final cell density (*SI Appendix*, Fig. S6), showing that the combination of increased membrane surface and Cat2 anchoring is generally beneficial. When strain BYa (Acc1m anchored) expressed both 2-PSPEX15 and Pex11, the specific TAL titer increased 5.9-fold relative to BY4741 (Fig. 3*B*), and the titer increased 3-fold reaching 553 ± 15 mg/L in 5-mL tube cultures (*SI Appendix*, Fig. S6). In this case, the final cell density was reduced by 40 to 50% relative to the BY4741 expressing these two genes (*SI Appendix*, Fig. S6), suggesting that it is the simultaneous expression of *PEX11* (smaller peroxisomes and increased membrane area) and anchoring of Acc1m that is creating this burden. Even so, both the TAL titer and the specific titer increased significantly. This may be due to the proximity and ease of metabolite shuttling between Acc1m and 2-PS on the smaller peroxisomes, as there is no increase in acetyl-CoA levels in these strains.

For our final strain BYac with all three enzymes anchored, TAL increased even further (as seen previously in Fig. 2*D*). However, in this case, overexpression of Pex11 was deleterious and significant drops in both the final cell density and the titer were observed (Fig. 3 and *SI Appendix*, Figs. S3 and S6. It is likely that we have now overwhelmed the peroxisome and further optimization is required. However, it is noteworthy that significant TAL increases were observed for strain BYa; this clearly highlights the power of *PEX11* upregulation for this colocalization strategy.

Discussion

In this study, we demonstrate the use of the native *S. cerevisiae* Pex15 anchoring motif for colocalization of enzymes on the peroxisomal membrane both to access an additional pool of acetyl-CoA and to increase metabolic pathway flux. We first tested peroxisomal display of the native Cat2 to intercept and convert exported acetyl-carnitine, resulting in a substantial increase in available acetyl-CoA. The results also highlight the directionality of Cat2 catalysis in the cytoplasm. The *CAT2* gene encodes for both the mitochondrial and peroxisomal Cat2 proteins, with transfer of the acetyl group from CoA to carnitine in the peroxisome, and the reverse in the mitochondria (35, 36). Based on our results, cytosolic expression of Cat2 favors the transfer reaction from carnitine to CoA, similar to the mitochondria. The local environment of Cat2 may play a role in the reaction direction favored, as the mitochondria and cytosol both have a lower pH (near neutral) than the alkaline peroxisomes (37, 38).

We then implemented this novel display method to create a protein metabolon consisting of the Cat2, Acc1m, and 2-PS enzymes required for TAL synthesis. Anchoring of the three enzymes enabled the use of the peroxisomal acetyl-CoA pool for efficient conversion to malonyl-CoA and then TAL. This led to a nearly 4.2-fold increase in the TAL titer relative to multicopy expression of 2-PS alone and a 6.9-fold increase over the initial low-copy system (Fig. 4). In our previous efforts to increase TAL synthesis in *S. cerevisiae*, promoter and plasmid modifications were used to obtain a titer of 0.25 g/L; subsequent improvements required extensive pathway engineering, 2-PS enzyme engineering,

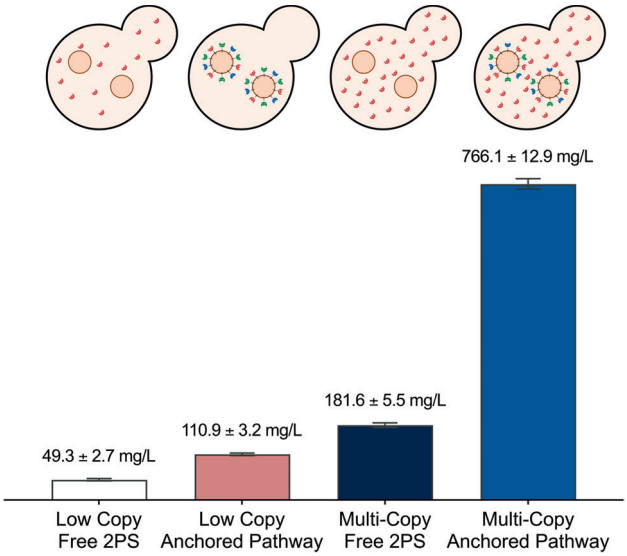

Fig. 4. Summary of engineering strategies to improve TAL synthesis via peroxisomal surface display in *S. cerevisiae*. Anchoring Cat2, Acc1m, and 2-PS (all low copy) increased TAL ~2-fold relative to unanchored 2-PS alone. With a multicopy plasmid for the limiting 2-PS, a >4-fold increase in TAL was observed for the fully anchored pathway relative to unanchored 2-PS. Bars represent mean ± 1-SD, $n = 3$ biological replicates.

and fed-batch cultivation (8, 9, 14). Our current results highlight the efficiency of peroxisomal surface display as we obtained 0.77 g/L prior to any extensive engineering efforts. Incorporation of our prior engineering strategies with peroxisomal surface display should further improve titers and yield.

We also explored varying the peroxisomal membrane surface area through the overexpression of the peroxisomal biogenesis protein Pex11, known to result in an increased number of smaller peroxisomes and to stimulate β-oxidation. For 2-PSPEX15 on a low-copy plasmid, TAL levels decreased (*SI Appendix*, Fig. S5) with *PEX11* overexpression and may reflect insufficient 2-PS levels for dimerization given the increased peroxisomal surface area. The multicopy 2μ 2-PSPEX15 plasmid rescued this drop, indicating sufficient dimerization with higher expression. In the absence of *PEX11* overexpression, no decrease in TAL levels was observed for 2-PSPEX15 relative to free-floating 2-PS for both low- and multicopy expression (*SI Appendix*, Figs. S3 and S4), suggesting dimerization is not an issue in the native Pex11 strains.

With two enzymes anchored (2-PS with either Cat2 or Acc1m), overexpression of *PEX11* resulted in significant increases in titers, demonstrating the advantages of reducing peroxisome size (and increasing membrane area) for our system. Anchoring all three enzymes while expressing *PEX11* reduced both growth and TAL titer. This may be due to detrimental effects on the native peroxisomal function (e.g., membrane transport functions) imposed by anchoring three different proteins on the now smaller peroxisomes. The genes for 2-PSPEX15 and Pex11 were both expressed using a strong constitutive promoter on a multicopy 2μ plasmid; intermediate expression of one or both enzymes would be a first step in improving the system. Although the overall peroxisomal surface expression system is not yet fully optimized, it is clear that this is a successful approach for increasing product titers and for pathway redirection in the cytosol, adding to the small list of cytosolic enzyme colocalization strategies available in *S. cerevisiae* (26). The anchoring of Cat2 also enables access to the peroxisomal acetyl-CoA pool; this should be broadly applicable for enhancing production of acetyl-CoA-based products.

Materials and Methods

Plasmid and Strain Construction. The plasmids and strains used in this work are listed in *SI Appendix*, Table S1 with primers summarized in *SI Appendix*, Table S2. All *S. cerevisiae* strains were built from BY4741 (39); all plasmids were built from pBT76 and pBT76-2μ (40). *Escherichia coli* strains used were XL1-Blue or DH5α (Invitrogen, Carlsbad, CA). Detailed methods for design and construction of plasmids and strains can be found in the *SI Appendix, Supplemental Methods*. Primers were synthesized by Integrated DNA Technologies (IDT, San Diego, CA). PCRs were performed using Q5® Hot Start High-Fidelity DNA Polymerase from New England Biolabs (NEB, Ipswich, MA) in a T100 Thermal Cycler from Bio-Rad (Hercules, CA). Gibson assembly reactions were performed using the NEBuilder® HiFi DNA Assembly Master Mix (NEB) and ligation reactions used T4 DNA Ligase (NEB). All restriction enzymes used for plasmid construction were purchased from NEB. All plasmids, gene disruptions, and cassette integrations were confirmed by Sanger sequencing (Azenta Life Sciences, South Plainfield, NJ) prior to use.

Media & Cultivation. *E. coli* strains XL-1 Blue and DH5α were cultivated in 5 mL lysogeny broth (LB) containing 150 μg/mL ampicillin for molecular cloning and plasmid maintenance. *S. cerevisiae* strains were grown at 30˚C in 15 × 125-mm borosilicate culture tubes containing 5 mL medium: YPD [10 g/L yeast extract (BD Difco™, BD, Franklin Lakes, NJ), 20 g/L peptone (BD Difco™), and 20 g/L D-glucose (Fisher Scientific, Hampton, NH)] prior to plasmid transformation, and selective SDC(A) [20 g/L D-glucose, 1.7 g/L yeast nitrogen base without amino acids (BD Difco™), 5 g/L casamino acids (BD Difco™), 100 mg/L adenine-hemisulfate (Sigma-Aldrich, St. Louis, MO), and 5 g/L ammonium sulfate (Fisher Scientific)] following transformation. Detailed yeast transformation methods can be found in *SI Appendix, Supplemental Methods*. For acetyl-CoA and TAL production, cells from overnight cultures in SDC(A) were reinoculated into SDC(A) (with 10 g/L D-glucose) and cultured for 48 or 96 h. Optical density (OD_{600}) was measured using a Shimadzu UV-2450 UV-Vis spectrophotometer (Shimadzu, Columbia, MD) and converted to cell density (gDCW/L) via a linear correlation. Cells were harvested by centrifugation at 3,000 rcf in a Beckman Coulter Allegra X-22R Centrifuge (Beckman Coulter, Brea, CA).

Extraction and Quantification of Acetyl-CoA. Acetyl-CoA was extracted from the cells using a cold-methanol quenching, a boiling ethanol protocol, and subsequent nitrogen-supported solvent evaporation based on previous methods (14, 41, 42), and assayed using the fluorometric Acetyl-CoA Assay Kit (Sigma-Aldrich, St. Louis, MO). Briefly, 5 mL yeast cultures were dropped into 25 mL of a 60% v/v methanol–water solution in a 50-mL conical tube that was prechilled to –40˚C; the culture was added to the center to avoid freezing on the tube wall. Cell-methanol suspensions were placed back at –40˚C for 5 min before pelleting at 1,800 rcf for 5 min. Cell pellets were resuspended in 5 mL of boiling ethanol-HEPES buffer (75% v/v ethanol, 0.25 M HEPES, pH 7.5). Suspensions were boiled for 3 min at 80˚C before nitrogen evaporation. Following complete solvent evaporation, cell pellets were resuspended in 100 μL of the assay kit buffer and centrifuged in a table-top microcentrifuge at 6,000 rcf for 5 min to remove the cell pellet. The fluorometric assay kit was used to quantify acetyl-CoA concentrations in the supernatant. Relative fluorescence was measured using 535-nm and 587-nm excitation and emission wavelengths in a SpectraMax M3 plate reader from Molecular Devices (San Jose, CA).

TAL Detection. Following harvest, 250 μL cell culture was centrifuged in a table-top microcentrifuge at 6,000 rcf for 5 min, and the supernatant collected for TAL analysis in a SpectraMax M3 plate reader. Absorbance was measured at 277 nm. TAL standards and samples were diluted 20:1 and 40:1 in ddH_2O, respectively, to ensure linearity.

Data, Materials, and Software Availability. All study data are included in the article and/or *SI Appendix*.

ACKNOWLEDGMENTS. This research was supported by the NSF (Grant No. CBET-1803677 and MCB-2013957) and a U.S. Department of Education GAANN Fellowship (to H.C.Y.). We thank Danielle Bever and Anhuy Pham for assisting with CRISPR-based integrations and screenings in yeast.

Author affiliations: [a]Department of Chemical and Biomolecular Engineering, University of California, Irvine, CA 92697-2580

1. S. M. Abdel-Aziz, M. M. Abo Elsoud, A. A. H. Anise, "Chapter 2 - Microbial biosynthesis: A repertory of vital natural products" in *Handbook of Food Bioengineering*, A. M. Grumezescu, A. M. B. T.-F. B. Holban, Eds. (Academic Press, 2017), pp. 25–54.
2. J. Du, Z. Shao, H. Zhao, Engineering microbial factories for synthesis of value-added products. *J. Ind. Microbiol. Biotechnol.* **38**, 873–890 (2011), 10.1007/s10295-011-0970-3.
3. J. Nielsen, J. D. Keasling, Engineering cellular metabolism. *Cell* **164**, 1185–1197 (2016), 10.1016/j.cell.2016.02.004.
4. J. Staunton, K. J. Weissman, Polyketide biosynthesis: A millennium review. *Nat. Prod. Rep.* **18**, 380–416 (2001), 10.1039/a909079g.
5. B. A. Pfeifer, C. Khosla, Biosynthesis of polyketides in heterologous hosts. *Microbiol. Mol. Biol. Rev.* **65**, 106–118 (2001). 10.1128/mmbr.65.1.106-118.2001.
6. E. S. Gomes, V. Schuch, E. G. de Macedo Lemos, Biotechnology of polyketides: New breath of life for the novel antibiotic genetic pathways discovery through metagenomics. *Braz. J. Microbiol.* **44**, 1007–1034 (2013).
7. K. J. Weissman, Chapter 1 introduction to polyketide biosynthesis. *Methods Enzymol.* **459**, 3–16 (2009).
8. J. Cardenas, N. A. Da Silva, Metabolic engineering of Saccharomyces cerevisiae for the production of triacetic acid lactone. *Metab. Eng.* **25**, 194–203 (2014), 10.1016/j.ymben.2014.07.008.
9. C. R. Vickery *et al.*, A coupled in vitro/in vivo approach for engineering a heterologous type III PKS to enhance polyketide biosynthesis in Saccharomyces cerevisiae. *Biotechnol. Bioeng.* **115**, 1394–1402 (2018), 10.1002/bit.26564.
10. M. Chia, T. J. Schwartz, B. H. Shanks, J. A. Dumesic, Triacetic acid lactone as a potential biorenewable platform chemical. *Green Chem.* **14**, 1850 (2012).
11. B. H. Shanks, P. L. Keeling, Bioprivileged molecules: Creating value from biomass. *Green Chem.* **19**, 3177–3185 (2017), 10.1039/c7gc00296c.
12. A. Krivoruchko, Y. Zhang, V. Siewers, Y. Chen, J. Nielsen, Microbial acetyl-CoA metabolism and metabolic engineering. *Metab. Eng.* **28**, 28–42 (2015), 10.1016/j.ymben.2014.11.009.
13. F. Pietrocola, L. Galluzzi, J. M. Bravo-San Pedro, F. Madeo, G. Kroemer, Acetyl coenzyme A: A central metabolite and second messenger. *Cell Metab.* **21**, 808–821 (2015). 10.1016/j.cmet.2015.05.014.
14. J. Cardenas, N. A. Da Silva, Engineering cofactor and transport mechanisms in Saccharomyces cerevisiae for enhanced acetyl-CoA and polyketide biosynthesis. *Metab. Eng.* **36**, 80–89 (2016), 10.1016/j.ymben.2016.02.009.
15. L. Sun *et al.*, Complete and efficient conversion of plant cell wall hemicellulose into high-value bioproducts by engineered yeast. *Nat. Commun.* **12**, 4795 (2021), 10.1038/s41467-021-25241-y.
16. W. H. Kunau, V. Dommes, H. Schulz, β-Oxidation of fatty acids in mitochondria, peroxisomes, and bacteria: A century of continued progress. *Prog. Lipid Res.* **34**, 267–342 (1995), 10.1016/0163-7827(95)00011-9.
17. X. Li *et al.*, Overproduction of fatty acids in engineered Saccharomyces cerevisiae. *Biotechnol. Bioeng.* **111**, 1841–1852 (2014), 10.1002/bit.25239.
18. Y. J. Zhou *et al.*, Harnessing yeast peroxisomes for biosynthesis of fatty-acid-derived biofuels and chemicals with relieved side-pathway competition. *J. Am. Chem. Soc.* **138**, 15368–15377 (2016), 10.1021/jacs.6b07394.
19. G. S. Liu *et al.*, The yeast peroxisome: A dynamic storage depot and subcellular factory for squalene overproduction. *Metab. Eng.* **57**, 151–161 (2020), 10.1016/j.ymben.2019.11.001.
20. S. Dusséaux, W. T. Wajn, Y. Liu, C. Ignea, S. C. Kampranis, Transforming yeast peroxisomes into microfactories for the efficient production of high-value isoprenoids. *Proc. Natl. Acad. Sci. U.S.A.* **117**, 31789–31799 (2020), 10.1073/pnas.2013968117.
21. C. W. T. Van Roermund, E. H. Hettema, M. Van Den Berg, H. F. Tabak, R. J. A. Wanders, Molecular characterization of carnitine-dependent transport of acetyl-CoA from peroxisomes to mitochondria in Saccharomyces cerevisiae and identification of a plasma membrane carnitine transporter, Agp2p. *EMBO J.* **18**, 5843–5852 (1999), 10.1093/emboj/18.21.5843.
22. A. Akşit, I. J. van der Klei, Yeast peroxisomes: How are they formed and how do they grow? *Int. J. Biochem. Cell Biol.* **105**, 24–34 (2018), 10.1016/j.biocel.2018.09.019.
23. N. Kulagina, S. Besseau, N. Papon, V. Courdavault, Peroxisomes: A new hub for metabolic engineering in yeast. *Front. Bioeng. Biotechnol.* **9**, 659431 (2021), 10.3389/fbioe.2021.659431.
24. A. Halbach *et al.*, Targeting of the tail-anchored peroxisomal membrane proteins PEX26 and PEX15 occurs through C-terminal PEX19-binding sites. *J. Cell Sci.* **119**, 2508–2517 (2006), 10.1242/jcs.02979.
25. Y. Elgersma *et al.*, Overexpression of Pex15p, a phosphorylated peroxisomal integral membrane protein required for peroxisome assembly in S. cerevisiae, causes proliferation of the endoplasmic reticulum membrane. *EMBO J.* **16**, 7326–7341 (1997), 10.1093/emboj/16.24.7326.
26. H. C. Yocum, A. Pham, N. A. Da Silva, Successful enzyme colocalization strategies in yeast for increased synthesis of non-native products. *Front. Bioeng. Biotechnol.* **9**, 606795 (2021), 10.3389/fbioe.2021.606795.
27. J. W. Choi, N. A. Da Silva, Improving polyketide and fatty acid synthesis by engineering of the yeast acetyl-CoA carboxylase. *J. Biotechnol.* **187**, 56–59 (2014).
28. Ł Opaliński, J. A. K. W. Kiel, C. Williams, M. Veenhuis, I. J. Van Der Klei, Membrane curvature during peroxisome fission requires Pex11. *EMBO J.* **30**, 5–16 (2011). 10.1038/emboj.2010.299.
29. Y. Y. C. Tam *et al.*, Pex11-related proteins in peroxisome dynamics: A role for the novel peroxin Pex27p in controlling peroxisome size and number in Saccharomyces cerevisiae. *Mol. Biol. Cell* **14**, 4089–4102 (2003). 10.1091/mbc.E03-03-0150.
30. S. Mindthoff *et al.*, Peroxisomal Pex11 is a pore-forming protein homologous to TRPM channels. *Biochim. Biophys. Acta Mol. Cell Res.* **1863**, 271–283 (2016), 10.1016/j.bbamcr.2015.11.013.
31. M. D. Mikkelsen *et al.*, Microbial production of indolylglucosinolate through engineering of a multi-gene pathway in a versatile yeast expression platform. *Metab. Eng.* **14**, 104–111 (2012), 10.1016/j.ymben.2012.01.006.
32. Y. Chen, J. Bao, I. K. Kim, V. Siewers, J. Nielsen, Coupled incremental precursor and co-factor supply improves 3-hydroxypropionic acid production in Saccharomyces cerevisiae. *Metab. Eng.* **22**, 104–109 (2014), 10.1016/j.ymben.2014.01.005.
33. A. A. Sibirny, Yeast peroxisomes: Structure, functions and biotechnological opportunities. *FEMS Yeast Res.* **16**, fow038 (2016), 10.1093/femsyr/fow038.
34. J. M. Jez *et al.*, Structural control of polyketide formation in plant-specific polyketide synthases. *Chem. Biol.* **7**, 919–930 (2000), 10.1016/S1074-5521(00)00041-7.

35. Y. Elgersma, C. W. T. Van Roermund, R. J. A. Wanders, H. F. Tabak, Peroxisomal and mitochondrial carnitine acetyltransferases of saccharomyces cerevisiae are encoded by a single gene. *EMBO J.* **14**, 3472–3479 (1995), 10.1002/j.1460-2075.1995.tb07353.x.
36. J. H. Swiegers, N. Dippenaar, I. S. Pretorius, F. F. Bauer, Carnitine-dependent metabolic activities in Saccharomyces cerevisiae: Three carnitine acetyltransferases are essential in a carnitine-dependent strain. *Yeast* **18**, 585–595 (2001), 10.1002/yea.712.
37. C. W. T. van Roermund *et al.*, The peroxisomal lumen in Saccharomyces cerevisiae is alkaline. *J. Cell Sci.* **117**, 4231–4237 (2004), 10.1242/jcs.01305.
38. V. A. Selivanov *et al.*, The role of external and matrix pH in mitochondrial reactive oxygen species generation. *J. Biol. Chem.* **283**, 29292–29300 (2008), 10.1074/jbc.M801019200.
39. C. B. Brachmann *et al.*, Designer deletion strains derived from Saccharomyces cerevisiae S288C: A useful set of strains and plasmids for PCR-mediated gene disruption and other applications. *Yeast* **14**, 115–132 (1998), 10.1002/(SICI)1097-0061(19980130)14:2<115::AID-YEA204>3.0.CO;2-2.
40. P. B. Besada-Lombana, *Strategies to Increase the Synthesis of Biorenewable Chemicals Derived from Second-Generation Feedstocks* (UC Irvine, 2018).
41. B. Gonzalez, J. François, M. Renaud, A rapid and reliable method for metabolite extraction in yeast using boiling buffered ethanol. *Yeast* **13**, 1347–1355 (1997), 10.1002/(SICI)1097-0061(199711)13:14<1347: AID-YEA176>3.0.CO;2-O.
42. S. G. Villas-Bôas, J. Højer-Pedersen, M. Åkesson, J. Smedsgaard, J. Nielsen, Global metabolite analysis of yeast: Evaluation of sample preparation methods. *Yeast* **22**, 1155–1169 (2005), 10.1002/yea.1308.